



Inhibition of STEP₆₁ ameliorates deficits in mouse and hiPSC-based schizophrenia models

Jian Xu¹, Brigham J. Hartley^{#5,8}, Pradeep Kurup^{#1}, Andre Phillips⁹, Aaron Topol^{5,8}, Meiyu Xu³, Chimezie Ononenyi¹, Ethan Foscue¹, Seok-Man Ho^{7,8}, Tyler D. Baguley², Nikisha Carty¹, Claudia S. Barros^{10,11}, Ulrich Müller¹⁰, Sounak Gupta¹², Peter A. Gochman¹³, Judith Rapoport¹³, Jonathan A. Ellman², Christopher Pittenger³, Bruce Aronow¹², Angus C. Nairn³, Michael W. Nestor⁹, Paul J. Lombroso^{1,3,4,*}, and Kristen J. Brennand^{5,6,8,*}

¹Child Study Center, Yale University, 230 South Frontage Rd, New Haven, CT, 06520

²Department of Chemistry, Yale University, 230 South Frontage Rd, New Haven, CT, 06520

³Department of Psychiatry, Yale University, 230 South Frontage Rd, New Haven, CT, 06520

⁴Department of Neurobiology, Yale University, 230 South Frontage Rd, New Haven, CT, 06520

⁵Department of Psychiatry, Icahn School of Medicine at Mount Sinai, New York, NY 10029

⁶Department of Neuroscience, Icahn School of Medicine at Mount Sinai, New York, NY 10029

⁷Department of Developmental and Stem Cell Biology, Icahn School of Medicine at Mount Sinai, New York, NY 10029

⁸Friedman Brain Institute, Icahn School of Medicine at Mount Sinai, New York, NY 10029

⁹Hussman Institute for Autism, 801 W. Baltimore St., Baltimore, MD 21201

¹⁰Dorris Neuroscience Center, Department of Cell Biology, The Scripps Research Institute, 10550 North Torrey Pines Road, La Jolla, CA 92037

¹¹Plymouth University School of Medicine, 16 Research Way PL6 8BU Plymouth UK

¹²UC Department of Pediatrics Cincinnati Children's Hospital Medical Center, 3333 Burnet Avenue, Cincinnati, Ohio 45229

Users may view, print, copy, and download text and data-mine the content in such documents, for the purposes of academic research, subject always to the full Conditions of use:http://www.nature.com/authors/editorial_policies/license.html#terms

***Corresponding authors**, Paul Lombroso: paul.lombroso@yale.edu, phone (203) 737-2224; Kristen J. Brennand: kristen.brennand@mssm.edu, phone (212) 659-8259 .

Supplementary Information accompanies the paper.

AUTHOR CONTRIBUTIONS

J.X. conducted biochemical experiments, behavioral tests and analyzed data. P.K. and N.C. conducted biochemical analyses. C.O. and E.F. conducted behavioral tests. M.X. and C.P. conducted PPI test and analyzed the data. J.R. contributed SZ2 fibroblasts. K.J.B. and B.J.H. reprogrammed the SZ1 and SZ2 hiPSC cohorts; K.J.B., B.J.H., and A.T. conducted SZ1- and SZ2-FB hiPSC neuronal differentiations; B.J.H. and S-M.H. completed *Ngn2*-inductions to yield SZ2-GLU hiPSC neurons; N.S. and K.S. contributed confocal microscopy of SZ1-FB and SZ2-GLU hiPSC neurons; S.G. and B.A. designed and conducted automated feature-based analysis of SZ1-FB and SZ2-GLU neuronal images; and A.P. and M.N. conducted SZ1-FB hiPSC neuron MEA. T.D.B. and J.A.E. provided TC-2153. C.B. and U.M. provided CNS-specific ErbB2/4 knockout brain lysates. J.X., P.J.L. and K.J.B. designed the experiments. J.X., A.C.N., P.J.L. and K.J.B. wrote the manuscript.

COMPETING FINANCIAL INTERESTS

The authors declare no competing financial interests.

¹³Childhood Psychiatry Branch, National Institute of Mental Health, National Institutes of Health, Bethesda, MD, USA.

These authors contributed equally to this work.

Abstract

The brain-specific tyrosine phosphatase, STEP (STriatal-Enriched protein tyrosine Phosphatase) is an important regulator of synaptic function. STEP normally opposes synaptic strengthening by increasing N-methyl D-aspartate glutamate receptors (NMDARs) internalization through dephosphorylation of GluN2B and inactivation of the kinases ERK1/2 and Fyn. Here we show that STEP₆₁ is elevated in the cortex in the *Nrg1*^{+/-} knockout mouse model of SZ. Genetic reduction or pharmacological inhibition of STEP prevents the loss of NMDA receptors from synaptic membranes and reverses behavioral deficits in *Nrg1*^{+/-} mice. STEP₆₁ protein is also increased in cortical lysates from the CNS-specific *ErbB2/4* mouse model of SZ, as well as in human induced pluripotent stem cell (hiPSC)-derived forebrain neurons and *Ngn2*-induced excitatory neurons from two independent SZ patient cohorts. In these selected SZ models, increased STEP₆₁ protein levels likely reflect reduced ubiquitination and degradation. These convergent findings from mouse and hiPSC SZ models provide evidence for STEP₆₁ dysfunction in SZ.

INTRODUCTION

STEP₆₁, a membrane-associated phosphatase found in the postsynaptic density¹ and endoplasmic reticulum², is highly expressed in the frontal cortex and other forebrain regions³. STEP₆₁ activity and degradation are tightly regulated through mechanisms that include inhibitory phosphorylation by PKA at a serine (ser221) within its substrate binding domain (kinase interacting domain; KIM)⁴ and degradation by the ubiquitin proteasome system (UPS)⁵. STEP₆₁ is the only STEP isoform detected in the cortex and is elevated in several neuropsychiatric disorders, including fragile X syndrome (FXS)⁶, Parkinson's disease (PD)⁷, and Alzheimer's disease (AD)⁵ (reviewed in^{8, 9}). The mechanisms for increased STEP₆₁ include increased translation (FXS), disrupted ubiquitination (PD), and beta-amyloid-mediated inhibition of the proteasome (AD). Amelioration of the biochemical, cognitive and behavioral deficits through either genetic reduction or pharmacological inhibition of STEP activity in mouse models support a causal relationship between elevated STEP₆₁ activity and these disorders^{8, 10, 11}.

We previously reported that STEP₆₁ is elevated in postmortem anterior cingulate cortex and dorsolateral prefrontal cortex of SZ patients, as well as in mice treated with the psychotomimetics (and NMDAR antagonists) MK-801 and phencyclidine (PCP)¹². Moreover, the acute (locomotor) and chronic (cognitive) effects of these psychotomimetics were blunted in STEP knock out (KO) mice¹².

Here we investigated the extent and effect of STEP₆₁ dysregulation in two genetic mouse models of SZ (*Nrg1*^{+/-} and CNS-specific *ErbB2/4* knockout mice^{13, 14}) as well as in two independent cohorts of SZ human induced pluripotent stem cell (hiPSC)-derived neurons. We not only observed increased STEP₆₁ activity in both genetic mouse models of SZ and the two cohorts of SZ hiPSC neurons, but also that STEP inhibition was sufficient to

ameliorate biochemical and behavioral deficits identified in these models. These results suggest a consistent and causally important contribution of STEP₆₁ to SZ pathophysiology and thus identify it as a plausible therapeutic target.

MATERIALS AND METHODS

hiPSCs

SZ1: All SZ1 fibroblasts were obtained from Coriell (P1 [GM02038, male], P2 [GM01792, male], P3 [GM01835, female], P4 [GM02497, male]). Control fibroblasts were obtained from ATCC (C1 [CRL-2522, male]) and Coriell (C2 [GM03440, male], C3 [GM03651, female], C4 [GM04506, female], C5 [AG09319, female], C6 [AG09429, female]). SZ2: The Rapoport laboratory at NIH generously provided SZ2 fibroblasts from nine cases with childhood-onset-SZ and eight controls (C1 [NSB553, male], C2 [NSB690, male], C3 [NSB2607, male], C4 [NSB3084, male], C5 [NSB3158, female], C6 [NSB3182, female], C7 [NSB3234, male], C8 [NSB3113, female], P1 [NSB499, female], P2 [NSB581, male], P3 [NSB676, female], P4 [NSB1442, male], P5 [NSB2513, male], P6 [NSB2620, male], P7 [NSB2011, female], P8 [NSB2476, female], P9 [NSB2962, male]). CNV analysis (SZ1¹⁵; SZ2¹⁶) indicates that there is no evidence for any large deletion of NRG1 (or related genes) in either cohort. Detailed description of patients and demographic summary can be found in SI Methods and SI Tables 1 and 2.

SZ1: Human fibroblasts (HFs) were reprogrammed using doxycycline-inducible lentiviral vectors¹⁵. SZ2: HFs were reprogrammed using Cytotune Sendai virus (Life Technologies). All hiPSC lines were validated by: long-term expansion beyond ten passages; FACS analysis for SSEA-4 and TRA-1-60 levels; transcript analysis for *OCT4*, *NANOG*, *c-MYC* and *LIN28*; and to confirm normal karyotypes (SI Figure 5a-c). Detailed description can be found in SI Methods.

hiPSC forebrain neural progenitor cells (NPCs) were derived, expanded and differentiated using established methods (SZ1: as described^{15, 17}; SZ2: as described^{18, 19} (detailed description can be found in SI Methods and validation SI Figure 5d). For *Ngn2*-induced neuronal differentiation, NPCs were transduced with a lentiviral TetO-mNgn2-T2A-PuroR (Addgene ID: 52047) together with a lentiviral constitutive reverse tetracycline transactivator (rtTA), (Addgene ID: 19780); transgene expression was induced with doxycycline (1 µg/ml; Sigma) for 7 days and selected with puromycin (1 µg/ml; Sigma) for 24 h. Detailed description can be found in SI Methods.

Rat cortical neurons

All experimental procedures were approved by the Yale University Institutional Animal Care and Use Committee and in strict accordance with the NIH Guide for the Care and Use of Laboratory Animals. Primary cortical neurons were isolated from rat E18 embryos as described^{11, 20}.

Mice

Nrg1^{+/-} mice were initially obtained from Mutant Mouse Regional Resource Centers supported by NIH (MMRRC Stock Number: 011745-UCD). Nrg1^{+/-} mice were backcrossed with C57BL/6 mice (Jackson Laboratory). All mice were genotyped using PCR according to the vendor's protocol. Brains from male Nrg1^{+/-} mice and littermates were collected at several time points (1, 3, 6, 9 and 12 months). All mice were maintained at a controlled temperature and 12 h light/dark cycle with regular diet. Brain lysates from ErbB2/4 CNS KO mice (9 months) were prepared as described¹⁴ and were kindly provided by Dr. Müller.

For biochemical testing, one group of Nrg1^{+/-} mice (male, 6-9 months) and WT littermates were administered intraperitoneally (i.p.) with vehicle (Veh, 0.1% DMSO in saline), clozapine (Clz, 1 mg/kg) or haloperidol (Hal, 2 mg/kg) daily for 2 weeks. A second group of Nrg1^{+/-} and WT mice were administered acutely with vehicle (Veh, 0.1% DMSO in saline) or TC-2153 (10 mg/kg) and sacrificed 3 h post injections. Frontal cortices were collected for biochemical analyses.

Genetic and pharmacological testing was done in distinct experiments; independent measurements are most appropriately compared within, rather than between, these experiments. For genetic reduction of STEP, Nrg1^{+/-} mice were crossed with STEP^{-/-} mice (on C57BL/6 background as described^{12, 21} to produce Nrg1^{+/-} mice null for STEP (double mutant); four cohorts was tested (6-9 months old, n = 9-16 each group). For pharmacologic reduction of STEP, mouse behavioral and cognitive assays were conducted on 4 cohorts of male Nrg1^{+/-} and WT littermates (6-9 months old, n = 9-16 each group) were used. Detailed methodology can be found in the SI Methods.

Reagents and antibodies

Reagents are detailed in SI Methods. Antibodies are listed in SI Table 4. Primers are listed in SI Table 5.

Data analysis

For Western blotting, phosphorylated protein levels were normalized to total protein levels, then to β -actin as loading control, with one exception: when pGluN2B was evaluated in synaptosomal fractions (P2), pGluN2B levels were normalized to β -actin directly. All data were expressed as means \pm SEM and statistical analyses were performed using SPSS Statistics 19 (IBM, New York, NY), Prism 6.0 (GraphPad Software, La Jolla, California) or JMP10 (SAS Institute Inc., Cary, North Carolina). Significance ($P < 0.05$) was determined by two-way analysis of variance (ANOVA) with post-hoc Bonferroni test. For locomotion, data were analyzed with two-way ANOVA with repeated measures, with post-hoc Bonferroni or paired t-test. A Chi-square one-sample t-test against 50% chance was used for social dominance tube test. For both SZ1 hiPSC studies (1-2 independent NPC lines were used per hiPSC, 1 hiPSC per individual (see SI Table 1)) and SZ2 hiPSC experiments (1 NPC line per hiPSC, 1 hiPSC per individual (see SI Table 2)), error bars represent variation (standard error) between parallel differentiations from the same NPC line.

RESULTS

STEP₆₁ is elevated in Nrg1^{+/-}, CNS-specific ErbB2/4 knockout mice and hiPSC neurons from SZ patients

NRG1^{13, 22, 23} and *ERBB4*²⁴ have been linked to SZ (reviewed in²⁵); either reduction or overexpression of Nrg1 signaling results in behavioral and cognitive deficits in animal models^{13, 26-28}. To investigate the functional implications of STEP₆₁ dysregulation in SZ, we analyzed STEP₆₁ protein levels in Nrg1^{+/-} and CNS-specific ErbB2/4 knockout mice^{13, 14}. Total STEP₆₁ was increased whereas the phosphorylated (inactive) form of STEP₆₁ was decreased in synaptosomal fractions (P2) from frontal cortex of Nrg1^{+/-} mice (Figure 1a). Phosphorylation of STEP₆₁ substrates GluN2B and ERK1/2, as well as synaptic levels of GluN2B, were decreased in P2 fractions (Figure 1a) in the presence of increased STEP₆₁. Analysis of the ratio of synaptic GluN2B versus total GluN2B also revealed a decrease in functional receptors in synaptic membranes (Figure 1a). There was a developmental increase in STEP₆₁ levels in Nrg1^{+/-} mice starting at 3 months of age (SI Figure 1a). A similar significant increase in STEP₆₁ was observed in ErbB2/4 CNS-specific knockout mice, another putative SZ model, with a decrease in the Tyr phosphorylation of GluN2B and ERK1/2 (SI Figure 1b).

We next examined a cohort of 6 controls and 4 SZ patients (herein referred to as cohort SZ1: available clinical information described in SI Table 1, originally described^{15, 17}), from which we had previously reprogrammed hiPSCs, differentiated hiPSC-derived neurons and reported synaptic deficits^{15, 29}. Gene expression comparisons of our hiPSC forebrain (FB) neuron populations to the Allen BrainSpan Atlas indicate that these cells, from both controls and SZ patients, resemble fetal rather than adult brain tissue, particularly the cortical and subcortical forebrain regions¹⁷. FB neuron populations are comprised of ~80% neurons and ~20% astrocytes¹⁵; moreover, the majority of FB neurons are VGLUT1-positive, and so are presumably glutamatergic, although approximately 30% are GAD67-positive (GABAergic) and a small minority are TH-positive (dopaminergic)^{15, 17}.

Perturbations in the GluN2A/GluN2B subunit ratio (encoded by the *GRIN2A* and *GRIN2B* gene) are thought to reflect synaptic deficits³⁰. Over the course of hiPSC FB neuronal differentiation, *GluN2A* expression increases with no change in *GluN2B*, resulting in an increased *GluN2A/GluN2B* mRNA ratio (SI Figure 2a). SZ1-FB neurons had a decreased *GluN2A/GluN2B* mRNA ratio (decreased expression of *GluN2A* while *GluN2B* was unchanged^{15, 17, 31}) (SI Figure 2b) and a decreased GluN2A/GluN2B protein ratio (decreased GluN2A protein in SZ1 FB neurons with no significant change in GluN2B protein levels) (SI Figure 2c-e).

We observed a significant increase of total STEP₆₁ (tSTEP₆₁) and active, non-phosphorylated STEP₆₁ (aSTEP₆₁) in SZ1-FB hiPSC neurons. Data are presented both by group average (Figure 1b) and by individuals (SI Figure 3). Increased STEP₆₁ was associated with decreased phosphorylation of GluN2B (Figure 1b; SI Figure 3c) and ERK1/2 (Figure 1b; SI Figure 3d) at the sites dephosphorylated by STEP. We also measured STEP₆₁ levels in patient fibroblasts, in patient-derived pluripotent hiPSCs, and in replicating hiPSC-derived NPCs. STEP₆₁ protein was not detected in fibroblast cultures and, although

present, showed no increase in SZ hiPSCs (SI Figure 4a, b) or NPC cultures (SI Figure 4c, d). These results indicate that the increase in STEP₆₁ is only detectable in post-mitotic SZ1-FB hiPSC neurons.

To validate these findings, we established a second cohort of SZ hiPSCs, comprising eight controls and nine SZ patients (herein referred to as SZ2: available clinical information described in SI Table 2; FACS validation for all hiPSCs (TRA-1-60 and SSEA4) and NPCs (NESTIN and SOX2) is shown in SI Figure 5; partially reported¹⁹). Consistent with our observations from SZ1, SZ2-FB hiPSC neurons showed increased total STEP₆₁ (Figure 1c; SI Figure 6a) and active STEP₆₁ (Figure 1c; SI Figure 6b), which correlated with decreased phosphorylation of GluN2B (Figure 1c; SI Figure 6c) and ERK1/2 (Figure 1c; SI Figure 6d). Moreover, because SZ2 hiPSCs were not generated using tetracycline-inducible methods, we were also able to apply a well-established *Ngn2*-induction method to yield populations of nearly pure excitatory (SZ2-GLU) neurons (SI Figure 7)^{32, 33}; critically, these *Ngn2*-induced GLU populations show no evidence for including GABAergic or dopaminergic neurons^{32, 33}. SZ2-GLU hiPSC neurons showed increased total (Figure 1d; SI Figure 8a) and active (Figure 1d; SI Figure 8b) STEP₆₁ levels, which again correlated with decreased phosphorylation of GluN2B (Figure 1d; SI Figure 8c) and ERK1/2 (Figure 1d; SI Figure 8d), indicating that increased STEP₆₁ could be specifically detected in defined populations of excitatory neurons derived from patients with SZ. Increased STEP₆₁ levels were driven by a subset of patients (a one-sample two-tailed t-test found that 3 of 4 of SZ1-FB, 4 of 9 of SZ2-FB and 3 of 9 of SZ2-GLU neuron samples tested showed evidence of elevated STEP₆₁ levels) (SI Table 3). Increased STEP activity in SZ2 GLU neurons in no way excludes the possibility that STEP levels are also perturbed in other neuronal or glial cell populations.

Genetic reduction of STEP₆₁ increases phosphorylation of STEP targets in *Nrg1*^{+/-} mice and hiPSC neurons

Nrg1^{+/-} mice null for STEP₆₁ (double mutant, DM) showed restored tyrosine phosphorylation levels of GluN2B and ERK1/2^{21, 34} (Figure 1e). Genetic reduction of *STEP* in *Nrg1*^{+/-} mice also rescued functional GluN2B-containing receptors at synaptic sites, as measured by synaptic versus total receptor levels (Figure 1e). Similarly, STEP₆₁ knockdown in hiPSC-derived neurons using lentiviral (LV)-short hairpin RNA (shRNA) reduced total (Figure 1f) and active (Figure 1g) STEP₆₁ levels in SZ1-FB hiPSC neurons, and increased phosphorylation of pGluN2B (Figure 1h) and pERK1/2 (Figure 1i).

Pharmacological inhibition of STEP increases phosphorylation of STEP targets in *Nrg1*^{+/-} mice and hiPSC neurons

Several neuroleptics including clozapine, risperidone, and haloperidol are known to result in inhibitory phosphorylation of STEP₆₁ by PKA¹². To test whether antipsychotic treatment was sufficient to reduce elevated STEP₆₁ activity in *Nrg1*^{+/-} mice, WT mice were administered vehicle (Veh), clozapine (Clz, 1 mg/kg, i.p.) or haloperidol (Hal, 2 mg/kg, i.p.) daily for 3 weeks. Indeed, Western blot analysis of P2 fractions demonstrated that in WT mice, neuroleptic treatment decreased STEP₆₁ activity without changing total STEP₆₁ levels, leading to an overall increase in the phosphorylation of STEP₆₁ substrates (Figure 2a). Similarly, neuroleptic treatment decreased STEP₆₁ activity without changing total STEP₆₁

levels in $Nrg1^{+/-}$ mice, leading to an overall increase in the phosphorylation of STEP₆₁ substrates, often above baseline WT levels (Figure 2a). These observations are in agreement with a previous finding that clozapine restores the tyrosine phosphorylation of GluN2B at Tyr¹⁴⁷² in $Nrg1^{+/-}$ mice³⁵. In both control and SZ1-FB hiPSC neurons, we similarly observed that 7-day treatment with clozapine (5 μ M) or loxapine (10 μ M) decreased STEP₆₁ activity and increased the phosphorylation GluN2B and ERK1/2, without affecting total STEP₆₁ levels (Figure 2b).

We recently characterized the dose-responses, time kinetics and specificity of a novel inhibitor of STEP [8-(trifluoromethyl)-1,2,3,4,5-benzo pentathiepin-6-amine hydrochloride], known as TC-2153¹¹. TC-2153 showed relative specificity for STEP₆₁, selectively inhibiting STEP in the cortex and hippocampus, but not two other closely related PTPs (i.e. PTP-SL in cerebellum and HePTP in spleen)¹¹. It also reversed the biochemical and cognitive deficits in a mouse model of AD¹¹, a disorder also characterized by a significant elevation of cortical and hippocampal STEP₆₁ levels¹⁰. TC-2153 treatment of both WT and $Nrg1^{+/-}$ mice produced increased tyrosine phosphorylation of GluN2B and ERK1/2 (Figure 2c). TC-2153 also inhibited STEP₆₁ activity in control and SZ1-FB hiPSC neurons, without changing total STEP₆₁ levels (Figure 2d). Treatment of control and SZ1-FB hiPSC neurons with 1 μ M TC-2153 led to an increase in the Tyr phosphorylation of pGluN2B and pERK1/2 (Figure 2d) that was comparable to clozapine or loxapine treatment (Figure 2b).

STEP inhibition increases spontaneous neuronal activity in control and SZ1-FB hiPSC neurons

We tested the effect of chronic 1 μ M TC-2153 treatment for 7 or 14 days on spontaneous neuronal activity in control and SZ1-FB hiPSC neurons using multi-electrode array (MEA) recordings. In two of the three SZ1 patients with elevated STEP₆₁ activity (see SI Figure 3 for relative STEP₆₁ levels in each patient), 14 days of administration with TC-2153 was sufficient to significantly increase the rate of neuronal firing in cells from these patients (Figure 3a, b). For one of the patients this was also true in the presence of acute (30 min) treatment with 50 μ M picrotoxin, a non-competitive channel blocker for the GABA_A receptor, indicating that changes resulting from TC-2153 may reflect changes to the glutamatergic network (Figure 3c-e).

STEP inhibition reverses behavioral and cognitive deficits in $Nrg1^{+/-}$ mice

We tested whether TC-2153 could reverse the behavioral and cognitive deficits in $Nrg1^{+/-}$ mice, which show increased locomotion and disrupted working memory and cognition^{13, 28}. First, we tested whether TC-2153 was effective in reversing PCP-induced hyperlocomotion in WT and $Nrg1^{+/-}$ mice. Following PCP administration (7.5 mg/kg, i.p.), a two-way ANOVA with repeated measures analysis demonstrated significant main effects of Time [5 min bin: $F(17,952) = 52.35$, $P < 0.0001$], Group [4 groups: $F(3,56) = 7.87$, $P < 0.001$] and a Time \times Group interaction [$F(51,952) = 1.78$, $P < 0.001$]. Bonferroni's *post hoc* test showed significant attenuation of PCP-induced hyperlocomotion in $Nrg1^{+/-}$ mice by TC-2153 ($P < 0.01$, compared to Veh-treated $Nrg1^{+/-}$ mice) (Figure 4a). Two-way ANOVA analysis of total distance traveled showed that there were significant effects of Treatment [Veh or

TC-2153, $F(1,54) = 20.73$, $P < 0.001$] and Genotype [WT or $Nrg1^{+/-}$, $F(1,54) = 4.92$, $P < 0.05$]. Bonferroni's *post hoc* test also revealed that TC-2153 led to a significant attenuation of PCP-induced hyperactivity in $Nrg1^{+/-}$ mice ($P < 0.01$, compared to Veh/ $Nrg1^{+/-}$ group (Figure 4b). In addition, pretreatment of Veh or TC-2153 had a significant effect on stereotypies (such as sniffing, rearing and grooming) [$F(1,55) = 21.67$, $P < 0.001$] and there was a significant main effect of Genotype [WT or $Nrg1^{+/-}$, $F(1,55) = 6.90$, $P < 0.05$]. Bonferroni's *post hoc* test revealed TC-2153 also attenuated PCP-induced stereotypies in $Nrg1^{+/-}$ mice ($P < 0.01$) (Figure 4c). TC-2153 (10 mg/kg, i.p.) also normalized locomotor activity in the open field (SI Figure 9a, b). Next we tested WT and $Nrg1^{+/-}$ mice in the Y-maze task. We found no difference in arm alternation in these mice (SI Figure 9c). However, we found $Nrg1^{+/-}$ mice made more arm entries indicating that $Nrg1^{+/-}$ mice were hyperactive in the Y-maze. Administration of TC-2153 reversed hyperactivity in the Y-maze (Figure 4d). Two-way ANOVA analysis of arm entries showed that there were significant effects of Treatment [Veh or TC-2153, $F(1,53) = 7.27$, $P < 0.01$] and Genotype [WT or $Nrg1^{+/-}$, $F(1,53) = 9.35$, $P < 0.01$]. Bonferroni's *post hoc* test showed that TC-2153 reduced arm entries in $Nrg1^{+/-}$ mice ($P < 0.05$, compared to Veh/ $Nrg1^{+/-}$ group (Figure 4d). Furthermore, TC-2153 reduced aggression in $Nrg1^{+/-}$ mice (Figure 4e), and significantly improved social behavior in a social novelty task (Figure 4f, g).

Because the motor abnormalities observed in $Nrg1^{+/-}$ mice (Fig 4a-c; SI Fig 9 a, b) may confound social behavioral measures, we next conducted a number of non-motor behavioral assays. Mice with deficits in $Nrg1$ signaling have been reported to show deficits in prepulse inhibition (PPI)^{36, 37}; we observed deficits in PPI in $Nrg1^{+/-}$ mice (SI Figure 9n). Repeated-measure ANOVA analyses revealed that TC-2153 normalized PPI (Figure 4h) with main effects of Treatment [Veh or TC, $F(1,18) = 11.43$, $P < 0.001$], Interval [30 ms or 100 ms, $F(1, 18) = 13.71$, $P < 0.001$] and Intensity [+6 db, +12 db or +16 db, $F(2,17) = 3.67$, $P < 0.05$]. TC-2153 treatment did not alter PPI in WT mice (SI Figure 9o). There was no difference in startle response in the different treatment groups (SI Figure 9p). TC-2153 also improved the ability of $Nrg1^{+/-}$ mice to distinguish between novel and familiar objects in the novel object recognition task (Figure 4i). Clozapine (1 mg/kg, i.p.), which served as a positive control, had similar significant effects in all tasks (SI Figure 10).

Our previous findings^{12, 38} suggested that genetic reduction of STEP was sufficient to reduce the biochemical and behavioral changes induced by the NMDAR antagonist PCP. To further demonstrate that pharmacological inhibition of STEP was sufficient to ameliorate the behavioral effects arising from NMDAR antagonism, we used another NMDAR blocker, MK-801, which has been widely validated as a pharmacological model of SZ and induces motor and cognitive deficits in mice³⁹⁻⁴¹. In agreement with previous reports^{42, 43}, we found MK-801 treatment induced hyperactivity (SI Figure 11a-c) and memory deficits in the Y-maze and novel object recognition tasks (SI Figure 11d, e); these deficits were significantly reversed by pretreatment with TC-2153 (SI Figure 11a-e). While MK-801 led to reduced GluN2B/GluN1 in synaptosomal membranes (P2) and decreased phosphorylation of ERK1/2, this was completely rescued by TC-2153 (SI Figure 11f).

We tested whether genetic reduction of STEP₆₁ in $Nrg1^{+/-}$ mice would recapitulate the effects of TC-2153. $Nrg1^{+/-}$ mice were hyperactive in the open-field test; this hyperactivity

was reduced in DM mice (SI Figure 12a, b). *Nrg1*^{+/-} hyperactivity after PCP administration, was significantly reduced in DM mice (SI Figure 12c-e). In the social dominance task, aggressiveness in *Nrg1*^{+/-} mice was normalized in DM mice (SI Figure 12f). In a Y-maze test of working memory, *Nrg1*^{+/-} mice were normal in terms of alternation choices (SI Figure 10c), but made significantly more arm entries; this was normalized in DM mice (SI Figure 12g, h). In the novel object recognition task, *Nrg1*^{+/-} mice failed to distinguish between novel and familiar objects, while DM mice behaved similarly to WT mice (SI Figure 12i). Finally, deficient social recognition in *Nrg1*^{+/-} mice was normalized in DM mice (SI Figure 13). Taken together, these experiments establish that both genetic reduction and pharmacological inhibition of STEP attenuate the biochemical, behavioral and cognitive deficits in *Nrg1*^{+/-} mice.

NRG1 signaling leads to ubiquitination and degradation of STEP₆₁ in rat cortical neurons and hiPSC neurons

STEP₆₁ mRNA levels were not different in SZ1-FB hiPSC neurons as measured using quantitative real-time PCR (SI Figure 14a), suggesting that increased transcription of STEP does not contribute to the elevation of STEP₆₁ protein levels in these neurons. Likewise, there was no detectable increase in STEP₆₁ mRNA in *Nrg1*^{+/-} mice (SI Figure 14b).

Because STEP₆₁ is normally regulated by the UPS, a process that is disrupted in SZ¹², PD⁷ and AD mouse models^{10, 44}, we tested the hypothesis that disruption of STEP₆₁ ubiquitination contributed to the elevated STEP₆₁ levels seen in our several SZ models. We observed decreased ubiquitination of total STEP₆₁ in SZ1-FB hiPSC neurons (Figure 5a), SZ2-FB hiPSC neurons (Figure 5b), and SZ2-GLU hiPSC neurons (Figure 5c). There was a general decrease of ubiquitinated proteins (SI Figure 15a) and perturbed levels in some (UBE2N, UBA6) UPS proteins in SZ1-FB hiPSC neurons (SI Figure 15c, e, g, i, k). Similarly, we observed decreased ubiquitination of total STEP in frontal cortex from *Nrg1*^{+/-} mice (Figure 5d). Here, while we did not observe a general decrease of ubiquitinated proteins (SI Figure 15b) or perturbations in most UPS proteins (SI Figure 15d, f, h, j, l), there was again a disruption of UBE2N levels (SI Figure 15d) in *Nrg1*^{+/-} mice.

We next asked if NRG1 signaling regulates STEP₆₁ levels. NRG1 β -treatment of WT rat cortical neurons (10 nM, 30 min) led to decreased STEP₆₁ levels; this was blocked by PD158780, a pan-ErbB receptor antagonist (Figure 5e). Concomitant with decreased STEP₆₁, there was increased tyrosine phosphorylation of GluN2B and ERK1/2 (Figure 5e) and increased surface levels of GluN2B and GluN1, all blocked by PD158780 (Figure 5f). The GABA_A receptor, which is not a STEP₆₁ substrate, showed no changes following NRG1 β treatment (Figure 5f). The NRG1 β extracellular domain (ECD) (50 ng/kg, i.p.) crosses the brain-blood barrier and is an effective activator of NRG1 signaling⁴⁵⁻⁴⁷. When injected into *Nrg1*^{+/-} mice (i.p.) daily for 5 consecutive days, NRG1 β ECD led to a significant reduction of STEP₆₁ and an increase in the tyrosine phosphorylation of the STEP₆₁ substrates GluN2B and ERK1/2 (Figure 5g). Similarly, NRG1 β -treatment of control and SZ1-FB hiPSC neurons resulted in a significant reduction of STEP₆₁ and an increase in the tyrosine phosphorylation of GluN2B and ERK1/2 (Figure 5h).

Finally, we examined whether NRG1 signaling can directly affect STEP₆₁ ubiquitination. NRG1 β -treatment (10 nM, 30 min) of WT rat cortical neurons increased ubiquitination (Figure 5i) and proteasome-dependent degradation (Figure 5i) of STEP₆₁. Although STEP₆₁ can be proteolysed by calpain after excitotoxic conditions²⁰, inhibition of calpain, caspase and lysozyme demonstrated that they were not involved in STEP₆₁ degradation (SI Figure 16). We repeated these experiments in SZ1-FB hiPSC neurons and assayed levels of STEP₆₁ ubiquitination after NRG1 β treatment. Consistent with our observations in rodents, NRG1 β treatment increased STEP₆₁ ubiquitination and degradation in both control and SZ1-FB hiPSC neurons (Figure 5j).

DISCUSSION

Here we demonstrate that STEP₆₁ protein levels are elevated in two mouse models of SZ (Nrg1^{+/-} and CNS-specific ErbB2/4 knockouts) as well as two populations of hiPSC-derived (FB and GLU) neurons from two independent cohorts of SZ patients (similarities and discrepancies between the mouse and human models are summarized in SI Table 6). Genetic or pharmacologic reduction of STEP₆₁ activity in both mouse and hiPSC-based SZ models increased the phosphorylation of STEP targets, altered neuronal activity and ameliorated cognitive and behavioral deficits. These results reveal a convergence of mouse and hiPSC studies, consistent with our previously reported post-mortem data¹² (although see⁴⁸). Elevated STEP₆₁ levels were driven by a subset (~50%) of our SZ1- and SZ2- hiPSC neurons; our results must next be replicated across larger cohorts of SZ patients, in order to better define the subset of patients with increased STEP₆₁ levels. We predict that, particularly for these individuals, STEP₆₁ inhibitors might be effective therapeutic agents.

Our mouse and hiPSC findings are consistent with the glutamate hypothesis of SZ (reviewed in⁴⁹⁻⁵¹); Nrg1 signaling is a critical mediator of synaptic function and plasticity in glutamatergic signaling (reviewed in²⁵) and Nrg1^{+/-} mice have been reported as having mEPSCs with faster decay and a smaller NMDA/AMPA ratio than wild-type littermates⁵². Deletion of ErbB4, the Nrg1^{+/-} receptor, results in reduced frequency and amplitude of mEPSCs⁵³. Finally, given that recombinant STEP protein decreased NMDAR currents and mEPSCs¹, while functional inhibition¹ or genetic deletion of STEP¹⁰ enhanced mEPSCs, and that activity-dependent regulation of STEP contributes to homeostatic stabilization of both NMDAR and AMPAR excitatory synapses⁵⁴, it is possible that perturbations in STEP₆₁ contribute to glutamatergic dysfunction both in mouse models of SZ and in patients. Nonetheless, this hypothesis needs to be investigated at the circuit-level in mouse models and confirmed by electrophysiology in hiPSC neurons.

Because genomic analyses have not linked variants at *PTPN5* (the gene encoding the protein STEP) to SZ, we posit that increased STEP₆₁ activity is a downstream biochemical consequence of other perturbations, rather than a primary cause of SZ. Increased STEP₆₁ levels seem to derive from disruptions in the ubiquitination and degradation of STEP₆₁, which are regulated, at least in part, by NRG1 signaling. This is consistent with evidence that genes involved in UPS are down-regulated in postmortem SZ cortical tissue^{55, 56}, and similar to what is observed in neurodegenerative diseases^{5, 7, 57}. While further work will clarify whether other mechanisms also affect STEP₆₁ protein levels, our findings suggest

that inhibition of STEP₆₁ activity might prove to be a promising point of therapeutic intervention for the subset of SZ patients in which STEP₆₁ levels are increased.

Supplementary Material

Refer to Web version on PubMed Central for supplementary material.

ACKNOWLEDGEMENTS

We thank laboratory members for helpful discussions and critical reading of the manuscript. This work was funded by NIH grants MH091037 and MH52711 (P.J.L), GM054051 (J.A.E), R01MH091861 (C.P), MH078833 (U.M), a Christopher & Dana Reeve Foundation fellowship (C.S.B), the Brain and Behavior Research Foundation (K.J.B), NIH grants MH101454 and MH106056 (K.J.B), as well as New York Stem Cell Foundation – Robertson Award (K.J.B). Kristen Brennand is a New York Stem Cell Foundation - Robertson Investigator.

As per our agreement with Coriell Cell Repository, some hiPSC lines generated from Coriell collection control and SZ fibroblasts will be available from Coriell. Additionally, all Coriell collection control and SZ hiPSCs have been deposited with the NIMH Center for Collaborative Studies of Mental Disorders at RUCDR, and all NIMH collection hiPSCs are currently being deposited.

REFERENCES

1. Pelkey KA, Askalan R, Paul S, Kalia LV, Nguyen TH, Pitcher GM, et al. Tyrosine phosphatase STEP is a tonic brake on induction of long-term potentiation. *Neuron*. 2002; 34(1):127–138. [PubMed: 11931747]
2. Bult A, Zhao F, Dirx R Jr, Sharma E, Lukacs E, Solimena M, et al. STEP61: a member of a family of brain-enriched PTPs is localized to the endoplasmic reticulum. *J Neurosci*. 1996; 16(24):7821–7831. [PubMed: 8987810]
3. Boulanger LM, Lombroso PJ, Raghunathan A, During MJ, Wahle P, Naegel JR. Cellular and molecular characterization of a brain-enriched protein tyrosine phosphatase. *J Neurosci*. 1995; 15(2):1532–1544. [PubMed: 7869116]
4. Paul S, Snyder GL, Yokakura H, Picciotto MR, Nairn AC, Lombroso PJ. The Dopamine/D1 receptor mediates the phosphorylation and inactivation of the protein tyrosine phosphatase STEP via a PKA-dependent pathway. *J Neurosci*. 2000; 20(15):5630–5638. [PubMed: 10908600]
5. Kurup P, Zhang Y, Venkitaramani DV, Xu J, Lombroso PJ. The role of STEP in Alzheimer's disease. *Channels*. 2010; 4(5):347–350. [PubMed: 20699650]
6. Goebel-Goody SM, Wilson-Wallis ED, Royston S, Tagliatela SM, Naegel JR, Lombroso PJ. Genetic manipulation of STEP reverses behavioral abnormalities in a fragile X syndrome mouse model. *Genes Brain Behav*. 2012; 11(5):586–600. [PubMed: 22405502]
7. Kurup P, Xu J, Videira RA, Ononenyi C, Baltazar G, Lombroso P, et al. STEP61 is a substrate of the E3 ligase parkin and is upregulated in Parkinson's disease. *Proc Natl Acad Sci U S A*. 2015; 112(4):1202–1207. [PubMed: 25583483]
8. Goebel-Goody SM, Baum M, Paspalas CD, Fernandez SM, Carty NC, Kurup P, et al. Therapeutic implications for striatal-enriched protein tyrosine phosphatase (STEP) in neuropsychiatric disorders. *Pharmacol Rev*. 2012; 64(1):65–87. [PubMed: 22090472]
9. Karasawa T, Lombroso PJ. Disruption of striatal-enriched protein tyrosine phosphatase (STEP) function in neuropsychiatric disorders. *Neurosci Res*. 2014
10. Zhang Y, Kurup P, Xu J, Carty N, Fernandez SM, Nygaard HB, et al. Genetic reduction of striatal-enriched tyrosine phosphatase (STEP) reverses cognitive and cellular deficits in an Alzheimer's disease mouse model. *Proc Natl Acad Sci U S A*. 2010; 107(44):19014–19019. [PubMed: 20956308]
11. Xu J, Chatterjee M, Baguley TD, Brouillette J, Kurup P, Ghosh D, et al. Inhibitor of the tyrosine phosphatase STEP reverses cognitive deficits in a mouse model of Alzheimer's disease. *PLoS Biol*. 2014; 12(8):e1001923. [PubMed: 25093460]

12. Carty NC, Xu J, Kurup P, Brouillette J, Goebel-Goody SM, Austin DR, et al. The tyrosine phosphatase STEP: implications in schizophrenia and the molecular mechanism underlying antipsychotic medications. *Transl Psychiatry*. 2012; 2:e137. [PubMed: 22781170]
13. Stefansson H, Sigurdsson E, Steinthorsdottir V, Bjornsdottir S, Sigmundsson T, Ghosh S, et al. Neuregulin 1 and susceptibility to schizophrenia. *Am J Hum Genet*. 2002; 71(4):877–892. [PubMed: 12145742]
14. Barros CS, Calabrese B, Chamero P, Roberts AJ, Korzus E, Lloyd K, et al. Impaired maturation of dendritic spines without disorganization of cortical cell layers in mice lacking NRG1/ErbB signaling in the central nervous system. *Proc Natl Acad Sci U S A*. 2009; 106(11):4507–4512. [PubMed: 19240213]
15. Brennand KJ, Simone A, Jou J, Gelboin-Burkhart C, Tran N, Sangar S, et al. Modelling schizophrenia using human induced pluripotent stem cells. *Nature*. 2011; 473(7346):221–225. [PubMed: 21490598]
16. Ahn K, Gotay N, Andersen TM, Anvari AA, Gochman P, Lee Y, et al. High rate of disease-related copy number variations in childhood onset schizophrenia. *Mol Psychiatry*. 2014; 19(5):568–572. [PubMed: 23689535]
17. Brennand K, Savas JN, Kim Y, Tran N, Simone A, Hashimoto-Torii K, et al. Phenotypic differences in hiPSC NPCs derived from patients with schizophrenia. *Mol Psychiatry*. 2015; 20(3):361–368. [PubMed: 24686136]
18. Lee IS, Carvalho CMB, Douvaras P, Ho SM, Hartley BJ, Zuccherato LW, et al. Characterization of molecular and cellular phenotypes associated with a heterozygous CNTNAP2 deletion using patient-derived hiPSC neural cells. *NPJ Schizophr*. 2015; 1:15019. [PubMed: 26985448]
19. Topol A, Zhu S, Hartley BJ, English J, Hauberg ME, Tran N, et al. Dysregulation of miRNA-9 in a Subset of Schizophrenia Patient-Derived Neural Progenitor Cells. *Cell Rep*. 2016; 15(5):1024–1036. [PubMed: 27117414]
20. Xu J, Kurup P, Zhang Y, Goebel-Goody SM, Wu PH, Hawasli AH, et al. Extrasynaptic NMDA receptors couple preferentially to excitotoxicity via calpain-mediated cleavage of STEP. *J Neurosci*. 2009; 29(29):9330–9343. [PubMed: 19625523]
21. Venkitaramani DV, Paul S, Zhang Y, Kurup P, Ding L, Tressler L, et al. Knockout of striatal enriched protein tyrosine phosphatase in mice results in increased ERK1/2 phosphorylation. *Synapse*. 2009; 63(1):69–81. [PubMed: 18932218]
22. Yang JZ, Si TM, Ruan Y, Ling YS, Han YH, Wang XL, et al. Association study of neuregulin 1 gene with schizophrenia. *Mol Psychiatry*. 2003; 8(7):706–709. [PubMed: 12874607]
23. Munafo MR, Thiselton DL, Clark TG, Flint J. Association of the NRG1 gene and schizophrenia: a meta-analysis. *Mol Psychiatry*. 2006; 11(6):539–546. [PubMed: 16520822]
24. Del Pino I, Garcia-Frigola C, Dehorter N, Brotons-Mas JR, Alvarez-Salvado E, Martinez de Lagran M, et al. Erbb4 deletion from fast-spiking interneurons causes schizophrenia-like phenotypes. *Neuron*. 2013; 79(6):1152–1168. [PubMed: 24050403]
25. Mei L, Xiong WC. Neuregulin 1 in neural development, synaptic plasticity and schizophrenia. *Nat Rev Neurosci*. 2008; 9(6):437–452. [PubMed: 18478032]
26. Yin DM, Chen YJ, Lu YS, Bean JC, Sathyamurthy A, Shen C, et al. Reversal of behavioral deficits and synaptic dysfunction in mice overexpressing neuregulin 1. *Neuron*. 2013; 78(4):644–657. [PubMed: 23719163]
27. O'Tuathaigh CM, Babovic D, O'Sullivan GJ, Clifford JJ, Tighe O, Croke DT, et al. Phenotypic characterization of spatial cognition and social behavior in mice with 'knockout' of the schizophrenia risk gene neuregulin 1. *Neuroscience*. 2007; 147(1):18–27. [PubMed: 17512671]
28. Karl T, Duffy L, Scimone A, Harvey RP, Schofield PR. Altered motor activity, exploration and anxiety in heterozygous neuregulin 1 mutant mice: implications for understanding schizophrenia. *Genes Brain Behav*. 2007; 6(7):677–687. [PubMed: 17309661]
29. Yu DX, Di Giorgio FP, Yao J, Marchetto MC, Brennand K, Wright R, et al. Modeling hippocampal neurogenesis using human pluripotent stem cells. *Stem Cell Rep*. 2014; 2(3):295–310.
30. Cui Z, Feng R, Jacobs S, Duan Y, Wang H, Cao X, et al. Increased NR2A:NR2B ratio compresses long-term depression range and constrains long-term memory. *Sci Rep*. 2013; 3:1036. [PubMed: 23301157]

31. Topol A, Zhu S, Tran N, Simone A, Fang G, Brennand KJ. Altered WNT Signaling in Human Induced Pluripotent Stem Cell Neural Progenitor Cells Derived from Four Schizophrenia Patients. *Biol Psychiatry*. 2015; 78(6):e29–34. [PubMed: 25708228]
32. Ho SM, Hartley BJ, Tcw J, Beaumont M, Stafford K, Slesinger PA, et al. Rapid Ngn2- induction of Excitatory Neurons from hiPSC-Derived Neural Progenitor Cells. *Methods*. 2015; (15):30159–6. pii: S1046-2023.
33. Zhang Y, Pak C, Han Y, Ahlenius H, Zhang Z, Chanda S, et al. Rapid single-step induction of functional neurons from human pluripotent stem cells. *Neuron*. 2013; 78(5):785–798. [PubMed: 23764284]
34. Venkitaramani DV, Moura PJ, Picciotto MR, Lombroso PJ. Striatal-enriched protein tyrosine phosphatase (STEP) knockout mice have enhanced hippocampal memory. *Eur J Neurosci*. 2011; 33(12):2288–2298. [PubMed: 21501258]
35. Bjarnadottir M, Misner DL, Haverfield-Gross S, Bruun S, Helgason VG, Stefansson H, et al. Neuregulin1 (NRG1) signaling through Fyn modulates NMDA receptor phosphorylation: differential synaptic function in NRG1^{+/-} knock-outs compared with wild-type mice. *J Neurosci*. 2007; 27(17):4519–4529. [PubMed: 17460065]
36. Hong LE, Wonodi I, Stine OC, Mitchell BD, Thaker GK. Evidence of missense mutations on the neuregulin 1 gene affecting function of prepulse inhibition. *Biol Psychiatry*. 2008; 63(1):17–23. [PubMed: 17631867]
37. Karl T, Burne TH, Van den Buuse M, Chesworth R. Do transmembrane domain neuregulin 1 mutant mice exhibit a reliable sensorimotor gating deficit? *Behav Brain Res*. 2011; 223(2):336–341. [PubMed: 21605597]
38. Xu J, Kurup P, Baguley TD, Foscue E, Ellman JA, Nairn AC, et al. Inhibition of the tyrosine phosphatase STEP61 restores BDNF expression and reverses motor and cognitive deficits in phencyclidine-treated mice. *Cell Mol Life Sci*. 2016; 73(7):1503–1514. [PubMed: 26450419]
39. Olszewski RT, Janczura KJ, Ball SR, Madore JC, Lavin KM, Lee JC, et al. NAAG peptidase inhibitors block cognitive deficit induced by MK-801 and motor activation induced by d-amphetamine in animal models of schizophrenia. *Transl Psychiatry*. 2012; 2:e145. [PubMed: 22850437]
40. Nilsson M, Hansson S, Carlsson A, Carlsson ML. Differential effects of the N-methyl-d-aspartate receptor antagonist MK-801 on different stages of object recognition memory in mice. *Neuroscience*. 2007; 149(1):123–130. [PubMed: 17826918]
41. van der Staay FJ, Rutten K, Erb C, Blokland A. Effects of the cognition impairer MK-801 on learning and memory in mice and rats. *Behav Brain Res*. 2011; 220(1):215–229. [PubMed: 21310186]
42. Liljequist S, Ossowska K, Grabowska-Anden M, Anden NE. Effect of the NMDA receptor antagonist, MK-801, on locomotor activity and on the metabolism of dopamine in various brain areas of mice. *Eur J Pharmacol*. 1991; 195(1):55–61. [PubMed: 1829683]
43. Bardgett ME, Boeckman R, Krochmal D, Fernando H, Ahrens R, Csernansky JG. NMDA receptor blockade and hippocampal neuronal loss impair fear conditioning and position habit reversal in C57Bl/6 mice. *Brain Res Bull*. 2003; 60(1-2):131–142. [PubMed: 12725901]
44. Kurup P, Zhang Y, Xu J, Venkitaramani DV, Haroutunian V, Greengard P, et al. Abeta-mediated NMDA receptor endocytosis in Alzheimer's disease involves ubiquitination of the tyrosine phosphatase STEP61. *J Neurosci*. 2010; 30(17):5948–5957. [PubMed: 20427654]
45. Kastin AJ, Akerstrom V, Pan W. Neuregulin-1-beta1 enters brain and spinal cord by receptor-mediated transport. *J Neurochem*. 2004; 88(4):965–970. [PubMed: 14756818]
46. Kato T, Abe Y, Sotoyama H, Kakita A, Kominami R, Hirokawa S, et al. Transient exposure of neonatal mice to neuregulin-1 results in hyperdopaminergic states in adulthood: implication in neurodevelopmental hypothesis for schizophrenia. *Mol Psychiatry*. 2011; 16(3):307–320. [PubMed: 20142818]
47. Rosler TW, Depboylu C, Arias-Carrion O, Wozny W, Carlsson T, Hollerhage M, et al. Biodistribution and brain permeability of the extracellular domain of neuregulin-1-beta1. *Neuropharmacology*. 2011; 61(8):1413–1418. [PubMed: 21903113]

48. Lanz TA, Joshi JJ, Reinhart V, Johnson K, Grantham LE 2nd, Volfson D. STEP levels are unchanged in pre-frontal cortex and associative striatum in post-mortem human brain samples from subjects with schizophrenia, bipolar disorder and major depressive disorder. *PLoS One*. 2015; 10(3):e0121744. [PubMed: 25786133]
49. Coyle JT. NMDA receptor and schizophrenia: a brief history. *Schizophr Bull*. 2012; 38(5):920–926. [PubMed: 22987850]
50. Javitt DC, Schoepp D, Kalivas PW, Volkow ND, Zarate C, Merchant K, et al. Translating glutamate: from pathophysiology to treatment. *Sci Transl Med*. 2011; 3(102):102mr102.
51. Lin CH, Lane HY, Tsai GE. Glutamate signaling in the pathophysiology and therapy of schizophrenia. *Pharmacol Biochem Behav*. 2012; 100(4):665–677. [PubMed: 21463651]
52. Jiang L, Emmetsberger J, Talmage DA, Role LW. Type III neuregulin 1 is required for multiple forms of excitatory synaptic plasticity of mouse cortico-amygdala circuits. *J Neurosci*. 2013; 33(23):9655–9666. [PubMed: 23739962]
53. Ting AK, Chen Y, Wen L, Yin DM, Shen C, Tao Y, et al. Neuregulin 1 promotes excitatory synapse development and function in GABAergic interneurons. *J Neurosci*. 2011; 31(1):15–25. [PubMed: 21209185]
54. Jang SS, Royston SE, Xu J, Cavaretta JP, Vest MO, Lee KY, et al. Regulation of STEP61 and tyrosine-phosphorylation of NMDA and AMPA receptors during homeostatic synaptic plasticity. *Mol Brain*. 2015; 8(1):55. [PubMed: 26391783]
55. Arion D, Corradi JP, Tang S, Datta D, Boothe F, He A, et al. Distinctive transcriptome alterations of prefrontal pyramidal neurons in schizophrenia and schizoaffective disorder. *Mol Psychiatry*. 2015; 20(11):1397–1405. [PubMed: 25560755]
56. Vawter MP, Crook JM, Hyde TM, Kleinman JE, Weinberger DR, Becker KG, et al. Microarray analysis of gene expression in the prefrontal cortex in schizophrenia: a preliminary study. *Schizophr Res*. 2002; 58(1):11–20. [PubMed: 12363385]
57. Snyder EM, Nong Y, Almeida CG, Paul S, Moran T, Choi EY, et al. Regulation of NMDA receptor trafficking by amyloid-beta. *Nat Neurosci*. 2005; 8(8):1051–1058. [PubMed: 16025111]

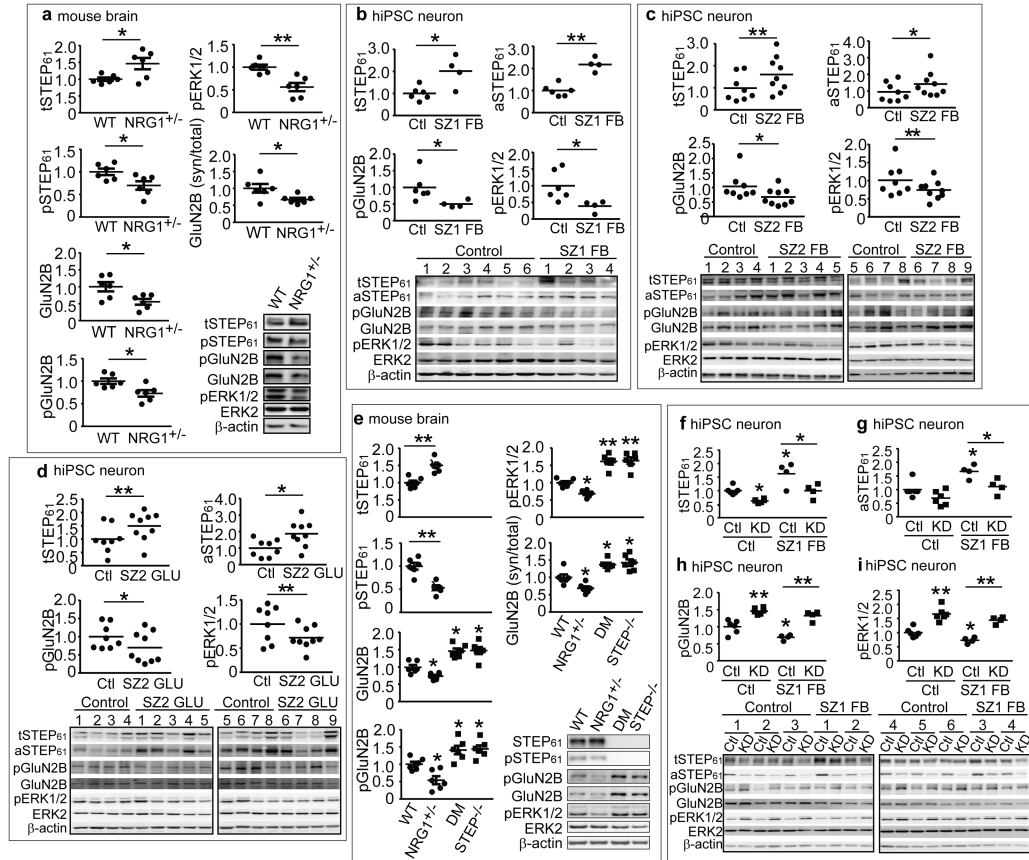


Figure 1. STEP₆₁ level is elevated in *Nrg1*^{+/-} mice and hiPSC neurons from SZ patients
(a) STEP₆₁ level is elevated in *Nrg1*^{+/-} mice. P2 membrane fractions from 9-month-old *Nrg1*^{+/-} mice were processed by western blotting (WB) using antibodies against total STEP₆₁, phosphorylated STEP₆₁ (pSTEP₆₁, inactive) and tyrosine phosphorylation of STEP substrates GluN2B and ERK1/2. All antibodies are listed in SI Table 4. **(b-d)** STEP₆₁ level is elevated in SZ patients-derived neurons. Total STEP₆₁ (tSTEP₆₁), active STEP₆₁ (aSTEP₆₁) and Tyr phosphorylation of STEP substrates (GluN2B and ERK1/2) levels were probed in SZ1 forebrain (FB) neurons **(b)**, SZ2-FB hiPSC neurons **(c)** and SZ2 *Ngn2*-induced excitatory (GLU) neurons **(d)**. Detailed description of patients and demographic summary can be found in SI Methods and SI Tables 1 and 2 **(e)** Tyr phosphorylation of STEP substrates is restored in *Nrg1*^{+/-} mice null for STEP. P2 fractions from wild type (WT), *Nrg1*^{+/-}, STEP^{-/-} and *Nrg1*^{+/-} STEP^{-/-} (double mutant, DM) mice were processed by WB and probed for targets shown in the figure. **(f-i)** STEP LV-shRNA knockdown (KD), relative to LV-scrambled control (Ctl), resulted in significantly decreased tSTEP₆₁ **(f)** and aSTEP₆₁ **(g)** levels and increased phosphorylation of the STEP₆₁ substrates pGluN2B **(h)** and pERK1/2 **(i)** in SZ1-FB hiPSC neurons. Mice data were expressed as mean ± SEM and statistical significance was determined using one-way ANOVA with Bonferroni test (**P* < 0.05, ***P* < 0.01, *n* = 6 each group). hiPSC neuron data were expressed as mean values from 3-6 replicates and statistical significance was determined by nested ANOVA analyses (**P* < 0.05, ***P* < 0.01, SZ1-FB: 6 controls and 4 patients; SZ2-FB and SZ2-GLU: 8 controls and 9 patients).

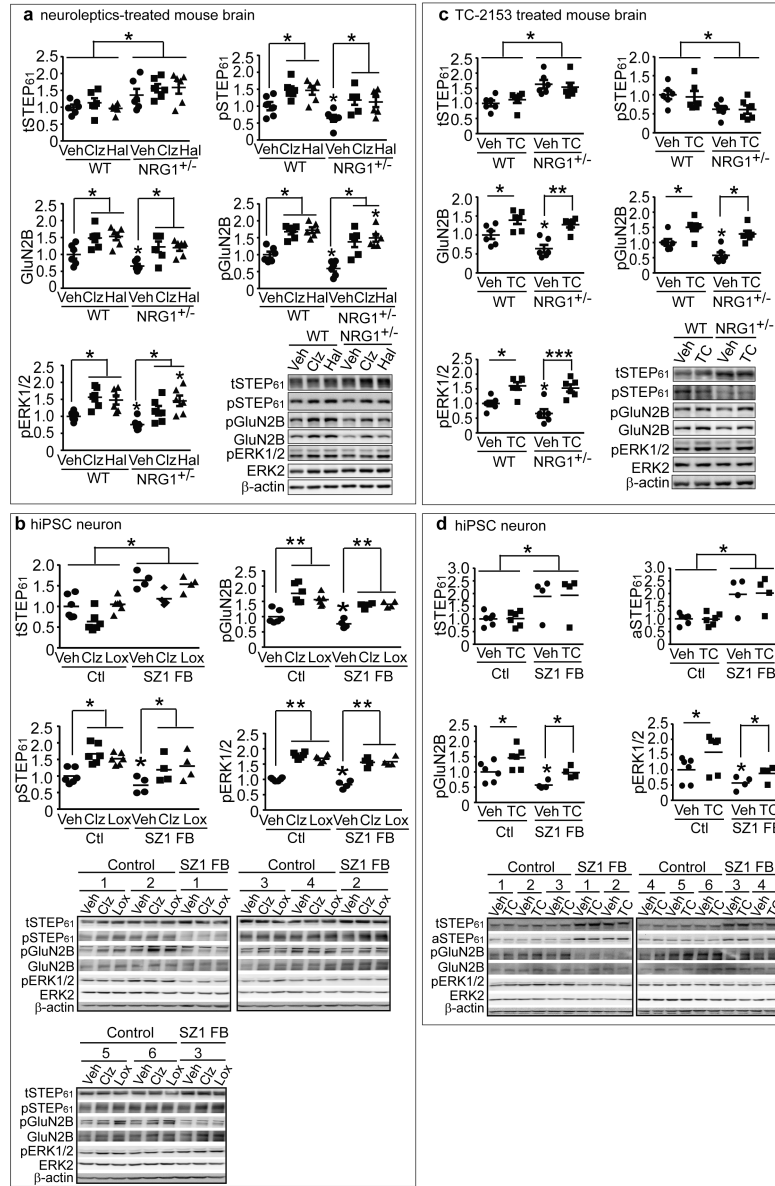


Figure 2. Pharmacological inhibition of STEP₆₁ restores NMDAR biochemical signaling in Nrg1^{+/-} mice and hiPSC neurons

(a) Antipsychotics administration leads to inactivation of STEP₆₁ and increases in Tyr phosphorylation of GluN2B and ERK1/2 *in vivo*. WT and Nrg1^{+/-} mice were administered clozapine (Clz, 1 mg/kg, i.p.), haloperidol (Hal, 2 mg/kg, i.p.) or vehicle (Veh) daily for 2 weeks. Changes in phosphorylation of STEP₆₁ and its substrates in P2 fractions were analyzed by WB. (b) Antipsychotics clozapine (Clz, 5 μM) and loxapine (Lox 10 μM) resulted in phosphorylation and inactivation of STEP₆₁ and subsequent increases in Tyr phosphorylation of GluN2B and ERK1/2 in control and SZ1-FB hiPSC neurons. (c) WT and Nrg1^{+/-} mice were administered TC-2153 (TC, 10 mg/kg, i.p.) or vehicle (Veh) acutely for 3 h. P2 fractions were used to probe for STEP and its substrates on WB. Mice data were expressed as mean ± SEM and statistical significance was determined using one-way

ANOVA with Bonferroni test (* $P < 0.05$, ** $P < 0.01$, # $P < 0.05$ compared with Nrg1^{+/-} Veh group, n = 6 each group). (d) TC-2153 treatment leads to significantly increased pGluN2B and pERK1/2 levels in control and SZ1-FB hiPSC neurons, without altering tSTEP₆₁ or aSTEP₆₁ levels. hiPSC neuron data were expressed as mean values from 3-6 replicates and statistical significance was determined by nested analyses using JMP (* $P < 0.05$, ** $P < 0.01$, SZ1-FB: 6 controls and 4 patients).

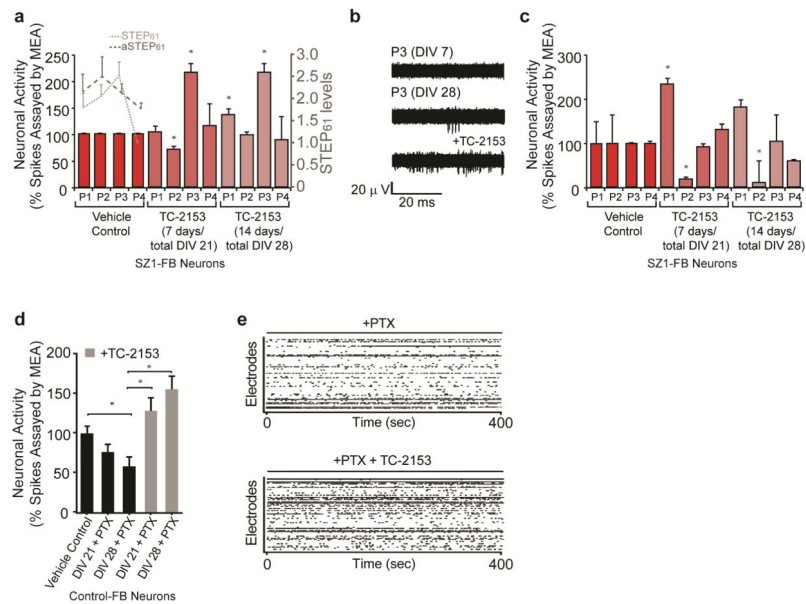


Figure 3. STEP inhibitor increases spontaneous neuronal activity in hiPSC neurons
(a) Multi-electrode array (MEA) analysis reveals that treatment with TC-2153 (1 μ M), for either the final 7 or 14 days of differentiation, increased the rate of spontaneous neuronal firing in SZ1-FB hiPSC neurons from the 2 patients with most elevated STEP₆₁ levels. **(b)** Representative raw MEA cumulative neuronal spike activity showing the effect of TC-2153 (1 μ M) on SZ1-FB hiPSC neurons. **(c)** Acute pharmacological inhibition of SZ1-FB hiPSC neurons with picrotoxin (PTX) (30 min, 50 μ M), when combined with MEA analysis, reveals that chronic TC-2153 (1 μ M) treatment (7 or 14 days) affects firing of excitatory neurons. **(d)** MEA analysis of one control hiPSC line, showing that acute PTX (50 μ M) treatment for 30 minutes results in decreased neuronal spiking, but when combined with chronic TC-2153 treatment (7 or 14 days), neuronal activity is increased compared to PTX treatment alone. **(e)** Representative raw MEA traces of neuronal activity showing the effect of TC-2153 (1 μ M), in the presence of PTX (50 μ M), on control hiPSC neurons. For all experiments, in each condition, 6 replicates per NPC line were tested (* $P < 0.05$, One-way ANOVA with Fisher’s post-hoc, SZ1-FB: 6 controls and 4 patients).

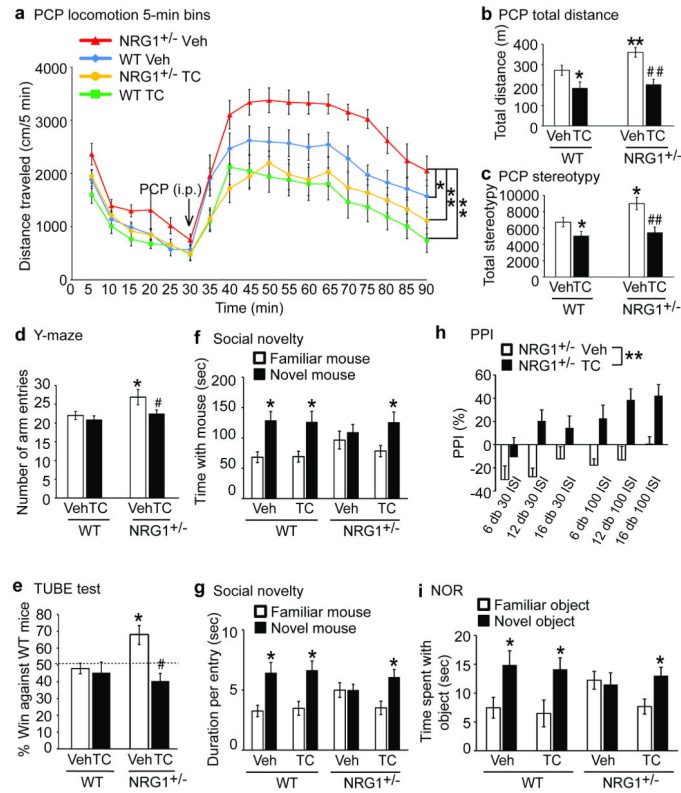


Figure 4. STEP inhibition reverses behavioral and cognitive deficits in *Nrg1*^{+/-} mice
 Male WT and *Nrg1*^{+/-} littermates (6-9 months old, 9-16 male mice each group) were used for all tests. **(a-c)** Pharmacological inhibition of STEP₆₁ normalizes PCP-induced hyperlocomotor activity and stereotypies. Mice were administered TC-2153 (TC, 10 mg/kg, i.p.) or vehicle (Veh), and monitored for basal activities for 30 min. Mice were then challenged with PCP (7.5 mg/kg, i.p.) for 1 h. Distance traveled in each 5 min bin during the 90 min test period **(a)**, total distance traveled **(b)** and total stereotypic counts **(c)** were recorded and analyzed using Activity Monitor (MED Associates). **(d)** *Nrg1*^{+/-} mice made more entries in Y-maze; this was reversed 3h after TC-2153 treatment. **(e)** TC-2153 administration normalizes aggressive behavior in *Nrg1*^{+/-} mice. Mice were administered TC-2153 (TC, 10 mg/kg, i.p.) or vehicle (Veh). Three h after injection, mice were tested in a narrow plastic tube against non-littermate naïve WT mice. Each mouse went through 4 trials and % win was plotted. **(f, g)** TC-2153 administration improves social behavior in the social novelty task in *Nrg1*^{+/-} mice. Mice were administered TC-2153 (TC, 10 mg/kg, i.p.) or vehicle (Veh). Three h after injection, mice were tested in 3-chamber social task. Behaviors in the first two stages (habituation and social preference) are shown in SI Figure 10. **(h)** TC-2153 treatment reversed PPI deficits in *Nrg1*^{+/-} mice. *Nrg1*^{+/-} mice were treated with TC or vehicle 3 h prior to PPI test. **(i)** TC-2153 reverses cognitive deficits in *Nrg1*^{+/-} mice in the novel object recognition (NOR) task. Mice were administered TC-2153 (TC, 10 mg/kg, i.p.) or vehicle (Veh). Three h after injection, mice were trained with two identical objects. Twenty-four h post training; mice were tested in the choice phase with one familiar object and one novel object. All data were expressed as mean ± SEM and statistical significance was determined using two-way ANOVA with repeated measures followed by post hoc

Bonferroni test for **(a)** or two-way ANOVA with post hoc Bonferroni test for **(b-d)** or repeated-measure (RM)-ANOVA for **(h)** or Chi-square one-sample t-test against 50% chance for **(e)** or Student t-test comparing two objects **(f, g, i)** (* $P < 0.05$, ** $P < 0.01$, compared with WT Veh group; ## $P < 0.01$ compared with Nrg1^{+/-} Veh group, n = 9-16 per group).

Author Manuscript

Author Manuscript

Author Manuscript

Author Manuscript

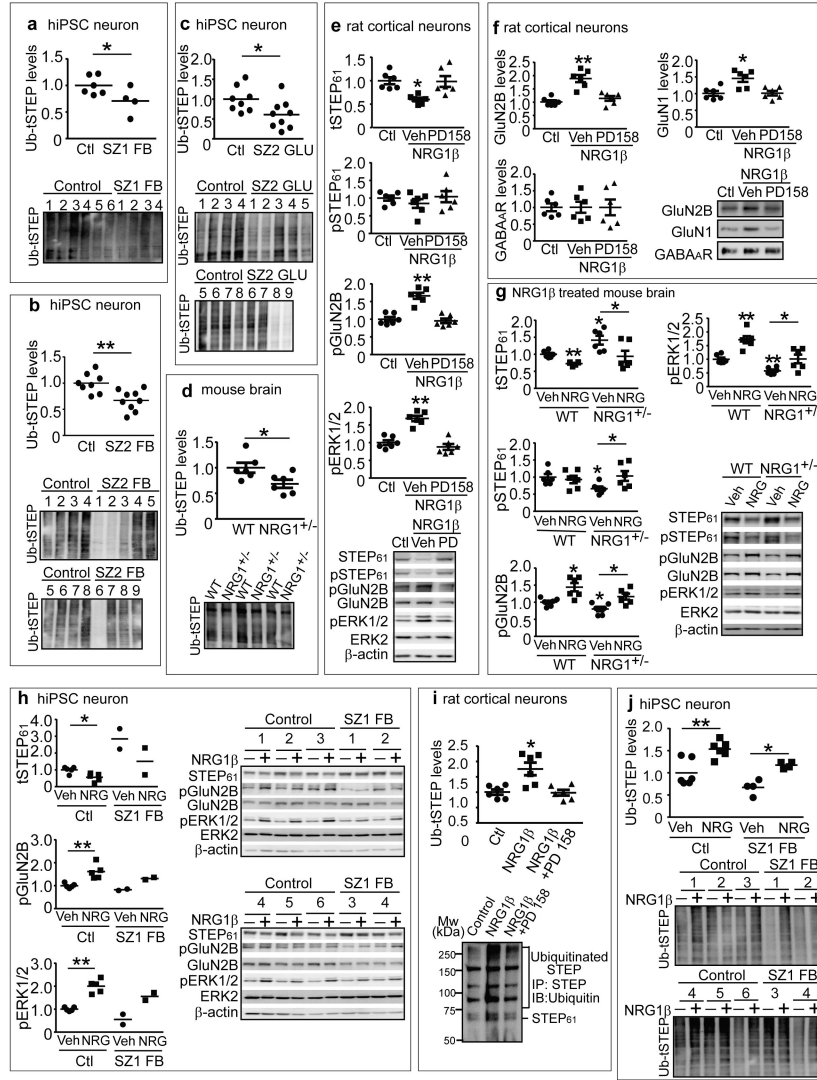


Figure 5. NRG1 signaling leads to ubiquitination and degradation of STEP₆₁ in rat cortical neurons and hiPSC neurons

(a-c) Ubiquitination of STEP is decreased in SZ hiPSC neurons. Ubiquitinated protein were pulled down from SZ1-FB hiPSC neurons (a), SZ2-FB hiPSC neurons (b) or SZ2-GLU hiPSC neurons (c) using tandem ubiquitin binding entities (TUBE) agarose beads as described in the SI Methods, followed by detecting using anti-STEP antibody. (d) Ubiquitination of STEP is decreased in *Nrg1*^{+/-} mice. Male WT and *Nrg1*^{+/-} mice (9 months old) were used to isolate ubiquitinated STEP using TUBE. (e) NRG1β treatment results in decreased STEP₆₁ level and increased Tyr phosphorylation of GluN2B and ERK1/2 in cultures. Rat cortical neurons (DIV 14) were pretreated with vehicle (0.1% DMSO) or pan-ErbB receptor antagonist (PD158780, 10 μM) for 30 min, followed by NRG1β (10 nM) for 30 min. Neuronal lysates were analyzed for STEP₆₁, pSTEP₆₁ and tyrosine phosphorylation of STEP substrates. (f) NRG1β treatment leads to increased surface NMDARs in cultures. Cortical neurons were treated with NRG1β (10 nM) for 30 min. Cells were incubated with 1.5 mg/ml Sulfo-NHS-SS-Biotin for 20 min at 4°C, lysed in 1xRIPA buffer. Equal amount

of lysates (300 μ g) was incubated with NeutrAvidin agarose to isolate biotinylated proteins including surface receptors. Total lysates were used to measure total protein levels. (g) NRG1 β administration normalizes STEP₆₁ level and restored Tyr phosphorylation of GluN2B and ERK1/2 in Nrg1^{+/-} mice. Male WT and Nrg1^{+/-} littermates (6-9 months old) were administered vehicle (saline) or NRG1 β ECD (50 ng/kg, i.p.) daily for 5 days. Frontal cortices were collected 3 h after the last injections and P2 fractions were used for biochemical analysis. (h) NRG1 β treatment results in decreased STEP₆₁ level and increased Tyr phosphorylation of GluN2B and ERK1/2 in human neurons. SZ1-FB and control neurons were treated with NRG1 β (10 nM) for 6 h. STEP₆₁ and phosphorylation of STEP substrates were assessed on WB. (i) NRG1 signaling leads to increased ubiquitination of STEP₆₁ in rat cortical neurons. Cultures were pretreated with MG-132 (10 μ M) for 1 h, followed by NRG1 β treatment (10 nM, 30 min). All STEP species were immunoprecipitated using anti-STEP antibody and probed with anti-ubiquitin antibody. (j) NRG1 β treatment leads to increased ubiquitination of STEP₆₁ in human neurons. SZ1-FB and control neurons were pretreated with MG-132 (10 μ M, 1 h), followed by NRG1 β treatment (10 nM, 6 h). Ubiquitinated STEP species were pulled down using TUBE and detected by anti-STEP antibody. All data were expressed as mean \pm SEM and statistical significance was determined using one-way ANOVA with Bonferroni test (* P < 0.05, ** P < 0.01, n = 6 each group).